Analytical Chloride Diffusion Model for Durability Assessment of Concrete-Lined Tunnels

P.L. Ng
The University of Hong Kong, Hong Kong, China

S.J. Zhou
BAE Australia, Queensland, Australia

J. Wang
Sun Yat-Sen University, Guangdong Province, China

doi: https://doi.org/10.21467/proceedings.171.15

ABSTRACT

The presence of chloride ion de-passivates reinforcing steel, thereby accelerating the corrosion of reinforcement and deterioration of reinforced concrete elements. Chloride ion diffusion constitutes the major deleterious factor undermining the durability of concrete-lined tunnels, especially tunnels through aquifers with high salinity. Hence, the service life prediction of concrete-lined tunnels should reliably take into account the chloride diffusivity in the concrete lining. Conventional serviceability design of reinforced concrete considers the exposure conditions in a categorical manner, with corresponding prescribed measures such as cover thickness and strength grade applied to the design. However, as a basis for quantitative assessment of durability, the chloride diffusion is generally dependent on the diffusivity of concrete, chloride ion concentration, environmental condition and the age. This paper devises an analytical chloride diffusion model with explicit formulation, which provides practical reference for adoption by design engineers. The application of the model is illustrated by examples of durability assessment of reinforced concrete tunnel lining.

1 INTRODUCTION

The corrosion of steel reinforcement in concrete is an electro-chemical reaction. Under the normal service conditions of reinforced concrete, the alkalinity of hydrated cement provides passivation for the embedded reinforcing steel, i.e. a passivating layer of oxide forms at the surface of reinforcing steel, thereby protecting the steel from corrosion (Mehta & Monteiro 2014). However, when chloride ion is present, the chloride ion activates the surface of steel to become the anode, whereas the passivated surface becomes the cathode. Such de-passivation by chloride ion sets up the electro-chemical cell and drastically accelerates the corrosion of reinforcing steel (Gjørv 2014). This in turn deteriorates the structural health and undermines the durability of reinforced concrete elements.

A variety of tunnels constitutes the lifeline infrastructure in urban settings. For concrete-lined tunnels, especially the tunnels through aquifers with high salinity, the deleterious effect of chloride ion on the durability and service life should be duly considered. In general, chloride ions could ingress into concrete by way of different transport mechanisms (Hooton 2014), including: a) diffusion of chloride through the pore water due to a chloride concentration gradient; b) permeation under a differential hydraulic pressure; c) absorption (sorption or convection) into unsaturated concrete due to a differential moisture concentration; and d) wick action with evaporation leaving high salt concentration at the drying front.

Among the aforementioned transport mechanisms, diffusion of chloride ions is the dominating mechanism practically (Wang et al. 2017). Thus, the durability assessment and service life prediction of concrete-lined tunnels should reliably take into account the chloride diffusion process in the concrete lining or concrete tunnel box structure. In conventional service life design of reinforced concrete, the exposure conditions are considered in a categorical manner, as exemplified by the exposure conditions of mild, moderate, severe, very severe, and abrasive (Buildings Department 2013). The European Standard adopts a more refined

Proceedings DOI: 10.21467/proceedings.171; Series: AIJR Proceedings; ISSN: 2582-3922; ISBN: 978-81-970666-7-2

categorization. In EN 206 (CEN 2013) and Eurocode 2 (CEN 2023), the exposure classes related to chloride induced corrosion are further designated into X0 (no risk of corrosion or attack), XD1 (moderate humidity), XD2 (wet, rarely dry), XD3 (cyclic wet and dry), XS1 (exposed to airborne salt but not in direct contact with seawater), XS2 (permanently submerged in seawater), and XS3 (tidal, splash and spray zones). With respect to the exposure classes, corresponding prescribed measures such as cover thickness, water to cement ratio and strength grade are applicable to the reinforced concrete design.

To more realistically and quantitatively assess the durability and service life of concrete construction, mathematical modelling of chloride diffusion has been formulated and applied (Shi et al. 2020). The chloride diffusion is generally dependent on the diffusivity of concrete and its rate of change, surface chloride ion concentration and its rate of change, environmental condition and the age. This paper devises an analytical chloride diffusion model with explicit formulation, which provides practical reference for adoption by design engineers. The application of the model is illustrated by examples of durability assessment of reinforced concrete tunnels.

2 CHLORIDE ION DIFFUSION MODELS

2.1 Fick's First Law

As a result of the physical phenomenon of Brownian motion, chloride ions in aqueous solution move randomly due to their frequent collisions with water molecules. Statistically, the random Brownian motion drives the chloride ions from high concentration zones to low concentration zones, eventually increasing the uniformity of the system (Freedman 1983). Such mass transfer of chloride ions from high to low concentration zones is referred to as chloride diffusion (Mauro 2021). The diffusion flux of chloride ions in aqueous solution is governed by Fick's First Law, as described in Equation (1) for typical one-dimensional diffusion process in a steady-state system (i.e. there is no change of chloride concentration at any point along the diffusion path).

$$J = -D\frac{\partial C}{\partial X} \tag{1}$$

where J = diffusion flux (or rate of mass transfer) through unit area in unit time (mol/m^{2}s), D = diffusion coefficient or diffusivity of chloride ions in aqueous solution (m^2/s), C = concentration of chloride ions (mol/m^3), and X = distance (m).

Fick's First Law determines that the diffusion flux has a linear relationship with the concentration gradient. Equation (1) is valid for concrete with a capillary pore water system. It is because the diffusion of chloride ions in solid cement paste is negligible, whereas diffusion of chloride ions does not occur in dry air or dry concrete without a connected capillary system of pore water.

2.2 Fick's Second Law

The change of chloride concentration in aqueous solution with time in the one-dimensional diffusion process is described by Fick's Second Law, as described in Equation (2) which reflects that the rate of chloride concentration change has a linear relationship with the second derivative of concentration function with respect to distance (Mauro 2021; Spiechowicz et al. 2023).

$$\frac{\partial C}{\partial t} = D\frac{\partial^2 C}{\partial X^2} \tag{2}$$

where t = time (s). It can be seen that time is related with Fick's Second Law but not with Fick's First Law.

Consider a semi-infinite homogenous medium with the finite face exposed to constant concentration of chloride source. Denote the initial chloride ion concentration in the medium to be C_0 as the initial condition, the solution of the above differential equation, i.e. Equation (2), is given by:

Proceedings DOI: 10.21467/proceedings.171
ISBN: 978-81-970666-7-2

Series: AIJR Proceedings
ISSN: 2582-3922

$$\frac{C-C_0}{C_s-C_0}=erfc\left(\frac{X}{2\sqrt{Dt}}\right) \tag{3}$$

where C_0 = initial chloride concentration, C_s = surface chloride concentration, and *erfc* = complementary error function. More information about the complementary error function is contained in the Appendix. Equation (3) can determine the change of chloride ion concentration with time at various distances from the exposed surface (Crank 1975). It should be noted that in the durability assessment of concrete elements, to predict the time to corrosion initiation and to evaluate the residual service life, the apparent chloride diffusivity estimated from the chloride profile is significantly influenced by the initial chloride concentration. A higher C_0 could yield a lower diffusivity, and consequently a longer time to corrosion initiation.

2.3 Time-variation of chloride diffusivity

Equation (3) is suitable for concrete with constant chloride diffusivity. In reality, the continual chemical reactions in concrete would gradually decrease the diffusivity and decelerate the rate of chloride ion ingress (Tang & Nilsson 1992). The decreasing chloride diffusivity could be accounted for via two approaches: a) to vary the instantaneous chloride diffusivity with time; and b) to adopt an apparent chloride diffusivity.

Regarding the first approach, the instantaneous chloride diffusivity is the diffusivity value obtained for concrete at a particular age and thus is valid only for that age (Wang et al. 2020). An empirical relationship between the diffusivity and age was put forward by Tang & Nilsson (1992), as expressed in Equation (4):

$$D_a=D_r\left(\frac{t_r}{t_a}\right)^m \tag{4}$$

where t_a = age of concrete (year), D_a = instantaneous chloride diffusivity at age t_a (m^2/s), t_r = reference concrete age at test or measurement (year), D_r = reference instantaneous chloride diffusivity at reference age t_r (m^2/s), and m = instantaneous age factor. The value of factor m is empirically dependent on the type of binder materials in the concrete mix and the mix proportioning. For example, for a concrete mix containing 25% pulverized fuel ash by mass as cement replacement, the corresponding value of m could be taken as 0.4; whereas for a concrete mix containing 25% pulverized fuel ash and 35% ground granulated blastfurnace slag by mass as cement replacement, the corresponding value of m could be taken as 0.6. Tang & Gulikers (2007) put forward a mathematical model based on decreasing chloride diffusivity, as formulated in the following:

$$\frac{C-C_0}{C_s-C_0}=erfc\left(\frac{X-\Delta X}{2\sqrt{\frac{D_c}{1-m}\left[\left(1+\frac{t_{e0}}{t_e}\right)^{1-m}-\left(\frac{t_{e0}}{t_e}\right)^{1-m}\right]\left(\frac{t_r}{t_e}\right)^m t_e}}\right) \tag{5}$$

where t_{e0} = age of concrete when exposure starts (year), t_e = duration of exposure (year), and ΔX = depth of convection zone (mm). It should be noted that $t_a = t_{e0} + t_e$. Regarding the depth of convection zone, it is to account for the case that the chloride concentration at concrete surface is not the highest but lower than that at a deeper zone, namely the surface convection zone whose depth is ΔX. Such phenomenon may occur when the chloride solution is repeatedly absorbed into the surface, followed by drying and evaporation of water leaving an increased chloride concentration which is not diffusion based, or when free chloride at surface is washed away by tide, splash or rain, or when carbonation of the near-surface concrete releases some bound or absorbed chloride. For concrete tunnels, the above circumstances are inapplicable or unlikely, so that ΔX could be nullified.

Regarding the second approach, the apparent chloride diffusivity is an approximate approach to determine an averaged or integrated diffusivity for a certain exposure period (Wang et al. 2019). It is evaluated based on

chloride profiles obtained after the exposure period by assuming a constant diffusivity for the period before the test (Bamforth 2004). Due to the sustained chemical reactions in concrete, the apparent chloride diffusivity would also decrease with age. Equation (6) denotes the mathematical expression.

$$D'_a = D'_r\left(\frac{t_r}{t_a}\right)^n \tag{6}$$

where D'_a = apparent chloride diffusivity at age t_a (m^2/s), D'_r = reference apparent chloride diffusivity at reference age t_r (m^2/s), and n = apparent age factor. The value of factor n is estimated from actual chloride profiles at various ages in the exposed concrete. The mathematical formulation of the apparent diffusivity model is given in the following:

$$\frac{C-C_0}{C_s-C_0} = erfc\left(\frac{X-\Delta X}{2\sqrt{D'_a t_e}}\right) = erfc\left(\frac{X-\Delta X}{2\sqrt{D'_r\left(\frac{t_r}{t_a}\right)^n t_e}}\right) \tag{7}$$

Typically, the decrease of chloride diffusivity of mature concrete is a gradual and long-term process that could sustain decades. By regression analysis of chloride profiles, the following relationships between D_a, D'_a, m and n have been yielded (Zhou 2018):

$$\frac{D_a}{D'_a} = m_4(\log t_a)^4 + m_3(\log t_a)^3 + m_2(\log t_a)^2 + m_1 \log t_a + m_0 \tag{8a}$$

$$\begin{pmatrix} m_0 \\ m_1 \\ m_2 \\ m_3 \\ m_4 \end{pmatrix} = \begin{pmatrix} -0.6895 \\ -0.2976 \\ 0.1717 \\ -0.0668 \\ 0.0118 \end{pmatrix} m + \begin{pmatrix} 0.9830 \\ -0.0081 \\ 0.0091 \\ -0.0013 \\ -0.0002 \end{pmatrix} \tag{8b}$$

$$\frac{D_a}{D'_a} = n_4(\log t_a)^4 + n_3(\log t_a)^3 + n_2(\log t_a)^2 + n_1 \log t_a + n_0 \tag{9a}$$

$$\begin{pmatrix} n_0 \\ n_1 \\ n_2 \\ n_3 \\ n_4 \end{pmatrix} = \begin{pmatrix} -0.7589 \\ -0.3295 \\ 0.1901 \\ -0.0738 \\ 0.0130 \end{pmatrix} n + \begin{pmatrix} 0.9943 \\ -0.0032 \\ 0.0062 \\ -0.0002 \\ -0.0004 \end{pmatrix} \tag{9b}$$

$$n = -0.1669m^2 + 1.0375m - 0.0052 \tag{10}$$

$$m = 0.2253n^2 + 0.9387n + 0.0073 \tag{11}$$

2.4 Time-variation of surface chloride concentration

The chloride ion concentration at the concrete surface, namely the extrados of lining or external side of tunnel box structure, is not constant but undergoes an accumulation or building-up process. Generally, two patterns

Proceedings DOI: 10.21467/proceedings.171
ISBN: 978-81-970666-7-2

Series: AIJR Proceedings
ISSN: 2582-3922

of surface chloride concentration variations with time could be found. They include the linear increase and square root increase patterns, as expounded hereunder.

With regard to the linear pattern, the relationship between surface chloride concentration and time in exposure is given by:

$$C_s - C_0 = k_1 t_e \tag{12}$$

where k_1 = gradient of linearly increasing surface chloride concentration (s^{-1}). The analytical model for chloride concentration *C'* at various depth and time follows Equation (13) and Equation (14), applicable when the chloride diffusivity is simultaneously decreasing (Zhou 2014):

$$C' = C_0 + k_1 t_e \left[(1+A) erfc\left(\sqrt{\frac{A}{2}}\right) - \sqrt{\frac{2}{\pi} A} \exp\left(\frac{-A}{2}\right) \right] \tag{13}$$

$$A = \frac{(X - \Delta X)^2 (1-m)}{2 D_r t_r^m \left[(t_e + t_{e0})^{1-m} - t_{e0}^{1-m} \right]} \tag{14}$$

With regard to the square root pattern, the relationship between surface chloride concentration and time in exposure is given by:

$$C_s - C_0 = k_2 t_e^{0.5} \tag{15}$$

where k_2 = gradient of square root increasing surface chloride concentration ($s^{-0.5}$). The analytical model for chloride concentration *C''* at various depth and time follows Equation (14) and Equation (16), applicable when the chloride diffusivity is simultaneously decreasing (Zhou 2016):

$$C'' = C_0 + k_2 t_e^{0.5} \left[\exp\left(\frac{-A}{2}\right) - \sqrt{\frac{A}{2}} erfc\left(\sqrt{\frac{A}{2}}\right) \right] \tag{16}$$

Dependent on the surrounding geo-environmental condition, the building-up of surface chloride concentration may resemble a linear, square root, or other pattern with variable gradients in general. From past experience, the accumulation of airborne chloride is relatively close to linear pattern, while the accumulation of chloride in wet-dry cycles and submerged conditions is relatively close to square root pattern. When the surface chloride concentration has built-up to a steady level, then C_s becomes constant and the mathematical model given by Equation (5) can be employed, with the exposure time substituted by an equivalent exposure time to account for the chloride profile attained during the surface chloride building-up process.

2.5 Effect of temperature

Since heat provides activation energy for diffusion, the temperature affects the chloride ion diffusion through altering the diffusivity. The effect of temperature on chloride diffusivity can be estimated according to the Arrhenius equation as follows (Laidler 1984):

$$D_T = D_{Tr} \exp\left[\frac{E_a}{R} \left(\frac{1}{T_r} - \frac{1}{T} \right) \right] \tag{17}$$

where T = temperature (K), D_T = chloride diffusion coefficient at temperature T, D_{Tr} = chloride diffusion coefficient at reference temperature T_r, E_a = activation energy of diffusion process (J/mol), and R = universal

gas constant which is equal to 8.314 JK^{-1}/mol. Taking the logarithm of both sides of Equation (17), it can be seen that the logarithm of chloride diffusion coefficient has a linear relation with the inverse of temperature.

$$\log D_T - \frac{E_a}{RT_r} = \log D_{Tr} - \frac{E_a}{RT} \tag{18}$$

Considering the diffusion near the cover zone of lining extrados or external side is of concern, the temperature of concrete thereat should be referred to. The value of E_a/R could be computed from Equation (19), with dependence on the water to cement ratio (W/C) of concrete (Page et al. 1981):

$$\frac{E_a}{R} = 1000\left[-52.5(W/C)^2 + 41.75(W/C) - 2.3\right] \tag{19}$$

3 EXPERIMENTAL MEASUREMENT OF CHLORIDE DIFFUSIVITY

In applying the chloride ion diffusion models, it is of prime importance to establish the chloride diffusivity of concrete. While concrete samples extraction from tunnels in service would be destructive and/or arise practicality concerns, representative samples could be prepared by casting specimens from the same concrete mixes as the tunnel lining or structure. Batch-by-batch differences from constituent materials could be eliminated by pre-planning the specimen preparation and testing during trial mixing, or minimized by replica sourcing of each ingredient for specimen preparation during post-construction or operation stage of the tunnel. There are different experimental methods to measure the chloride diffusivity of concrete, as outlined below.

3.1 Migration cell experiment

The testing methodology and procedures are specified in NT Build 355 (Nordtest 1997). Concrete cylinder of 100 mm diameter is cast and cured in water tank until 90 days of age. After curing, the cylinder is wiped with dry cloth and wait to attain surface-dry condition. The curved surface of the cylinder is coated with epoxy to achieve water impermeability. Concrete slices of 100 mm diameter and 50 mm thickness are cut from cylinder (during cutting, the top 10 mm portion of cylinder is discarded). The concrete slice is then placed into the migration cell, where one face of the slice is in contact with 5 wt.% NaCl solution (compartment 1 of the cell) whereas the opposite face of the slice is in contact with 1.2 wt.% NaOH solution (compartment 2 of the cell). A rubber sealant ring is fitted onto the epoxy-coated side (curved) surface to separate the two compartments.

The two half-cells are connected to a 12V fixed voltage D.C. (direct current) and an ammeter. The voltage drop ΔE across the slice specimen is measured with two reference electrodes each inserted into a compartment. The chloride concentration in compartment 2 is measured daily over one week to obtain the rate of change of chloride concentration. The chloride diffusivity is then obtained as:

$$D = \frac{RTh}{Fz\Delta EA}\left(\frac{V_2}{C_1}\right)\left(\frac{\Delta C_2}{\Delta t}\right) \tag{20}$$

where h = slice thickness (m), F = Faraday constant which is equal to 96485 C/mol, z = absolute value of valence of chloride ion (z = 1), ΔE = voltage drop across slice specimen (V), A = area of concrete slice (m^2), C_1 = chloride concentration in compartment 1, V_2 = volume of compartment 2 (m^3), and $\Delta C_2/\Delta t$ = rate of change of chloride concentration in compartment 2.

3.2 Accelerated chloride penetration

The methodology and procedures of accelerated chloride penetration test are described in NT Build 443 (Nordtest 1995). Concrete cylinder of 75 mm or 100 mm diameter is cast and water cured until 28 days of age. The cylinder is then cut into halves. Upon dried to surface-dry condition, all surfaces of half-cylinder except the cut face is coated with 1 mm thick epoxy or polyurethane coating. After the coating has hardened, the half-

Proceedings DOI: 10.21467/proceedings.171
ISBN: 978-81-970666-7-2

Series: AIJR Proceedings
ISSN: 2582-3922

cylinder specimen is immersed in 14 wt.% NaCl solution at 23°C ± 2°C for a period of 35 days with stirring of the chloride solution once per week. Subsequent to exposure to chloride solution, grinding is performed at the face of slice within a diameter of approximately 10 mm less than the diameter of cylinder (in order to avoid the influence of edge effect). At least 8 layers are to be ground off, with the outermost layer having a thickness of minimum 1.0 mm and each remaining layer sufficiently thick to yield at least 5 g of dry concrete dust. The depth of each layer from the exposed surface is re-measured at 5 points using caliper and averaged.

The acid-soluble chloride content of concrete dust sample from each layer is measured using Volhard titration method (Nordtest 1996) as detailed in the Appendix. This enables the determination of chloride concentration $C(X,t)$ at various depth X and time t. From the other half-cylinder, concrete slice of 20 mm is cut, and circa 20 g of concrete fragment sample is obtained by crushing. The acid-soluble chloride content of concrete fragment sample is measured using Volhard titration method as the initial chloride concentration C_0. By fitting of Equation (21) based on regression analysis, the values of C_s and D_e can be obtained:

$$C(X,t) = C_s - \frac{C_s - C_0}{erf\left(\frac{X}{2\sqrt{D_e t}}\right)} \tag{21}$$

where D_e = effective chloride diffusion coefficient (m^2/s). Given a selected value of reference chloride concentration C_r, say 0.05% by mass of concrete, the chloride penetration parameter K_{Cr} ($m/s^{0.5}$ or $mm/s^{0.5}$) corresponding to the selected C_r value can be evaluated in accordance with Equation (22):

$$K_{Cr} = \frac{2\sqrt{D_e}}{erf\left(\frac{C_s - C_r}{C_s - C_0}\right)} \tag{22}$$

3.3 Non-steady-state migration experiment

The methodology and procedures of the experiment are detailed in NT Build 492 (Nordtest 1999). Concrete cylinder of 100 mm diameter is cast, from which slice specimen of the same diameter and 50 mm thickness is cut. A silicone rubber sleeve is fitted onto the curved surface of slice specimen and secured with stainless steel ring clamp. The rubber sleeve is of 150 mm length and extends above the slice specimen. The assembly is placed on an inclined plastic support with plastic stud spacers, altogether put at the base of catholyte reservoir filled with 10 wt.% NaCl solution. The plastic spacers provide a gap for direct contact between the bottom face of concrete slice and NaCl solution. The rubber sleeve above the slice is filled with 1.2 wt.% NaOH solution, which becomes the anolyte solution in direct contact with the top face of concrete slice. A regulated voltage D.C. power supply is set up with the negative pole connected to a 0.5 mm thick stainless steel plate cathode and positive pole connected to a 0.5 mm thick stainless steel perforated plate or mesh anode.

The voltage is initially set as 30V and the initial current through the specimen is recorded upon turning on the power. Then, the voltage is adjusted within the range of 10V to 60V with respect to the initial current and the test is sustained for a duration ranging from 6 hours to 96 hours according to NT Build 492 (Nordtest 1999). After the test, the slice specimen is rinsed and split into two halves. Silver nitrate ($AgNO_3$) solution of 0.1 M concentration is sprayed onto the split surface of one half-slice and wait for circa 15 minutes until white silver chloride precipitation appears on the split surface. The chloride penetration depth is measured using caliper at 10 mm intervals (to avoid the influence of edge effect, measurement is not made within 10 mm from the edge) and averaged. The chloride diffusivity can be evaluated from Equation (23):

$$D_n = \frac{RTh}{Fz(U-2)t}\left[x_d - \sqrt{\frac{RTh x_d}{Fz(U-2)}}\frac{2}{erf(1-2r_C)}\right] \tag{23}$$

where D_n = non-steady-state migration coefficient (m^2/s), U = absolute value of applied voltage (V), x_d = average value of chloride penetration depth (m), r_C = ratio of chloride concentration at which the colour changes to chloride concentration in the catholyte solution (r_C is approximately equal to 0.07/2 = 0.035).

3.4 Rapid chloride permeability test

The methodology and procedures of rapid chloride permeability test (RCPT) are specified in American Standard AASHTO T 277 (AASHTO 2007). Concrete cylinder of 100 mm diameter is cast and cured until 56 days of age. Slice specimen of 100 mm diameter and 50 mm thickness is cut from the cylinder. A potential difference of 60V D.C. from a constant voltage power supply is maintained across the ends of slice specimen, one of which is immersed in 3.0 wt.% NaCl solution, and the other is immersed in 1.2 wt.% NaOH solution. The amount of electric current passing through the slice specimen during a 6-hour period is monitored using a voltmeter. The total charge passed is related to the resistance of the slice specimen to chloride ion penetration. Empirical relationship between the total charge passed and chloride diffusivity was recommended by Hooton et al. (1997), as given by Equation (24):

$$D = 0.3\times10^{-6}Q^2 + 0.6\times10^{-3}Q + 0.9375 \tag{24}$$

where Q = total charge passed (C).

3.5 Threshold chloride concentration

When the chloride concentration at the reinforcement surface reaches the threshold level, corrosion of reinforcing steel accelerates and is considered to enter into the corrosion propagation period. The values of threshold chloride concentration vary widely as reported in the literature (Angst and Vennesland 2009), and attention has to be paid regarding the expression of chloride component (free chloride or total chloride) and proportional basis (by mass of concrete or by mass of binder). According to Japanese Standard (Japan Society of Civil Engineers 1999), before the availability of a more reliable value, a threshold chloride concentration of 0.06% total chloride by mass of concrete may be used.

4 APPLICATIONS TO DURABILITY ASSESSMENT

4.1 Delineation of exposure period

To demonstrate the applications of chloride ion diffusion model, examples of durability assessment are presented hereunder. At the outset, to duly consider the time-variations of chloride diffusivity of concrete and surface chloride concentration in the analysis, the entire duration of chloride exposure is delineated into distinct time periods with different diffusion conditions. Figure 1 illustrates the delineation of exposure period, namely: a) period 1 (up to time t_I) during which the surface chloride concentration increases and diffusivity decreases; b) period 2 (up to time t_{II}) during which the surface chloride concentration is constant and diffusivity decreases; and c) period 3 during which the surface chloride concentration and diffusivity are both constant.

Proceedings DOI: 10.21467/proceedings.171
ISBN: 978-81-970666-7-2

Series: AIJR Proceedings
ISSN: 2582-3922

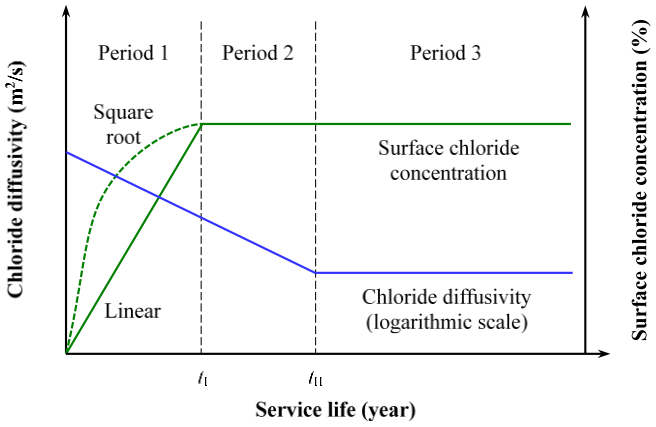

Figure 1: Delineation of exposure period

Equations (13) and (16) are applicable to period 1 but not to subsequent periods. Instead, in period 2, an equivalent exposure time for period 2 ($t_{eq\wedge I}$) having a similar profile at the joint time with Period 1 is introduced: $t_{eq\wedge I} = t_e - \Delta t_{eq\wedge I}$, where $\Delta t_{eq\wedge I}$ is the time difference between period 2 and period 1 with matching chloride profiles (year). With a linearly increasing surface chloride concentration during period 1, the chloride concentration in period 2 is given by:

$$C'_{II} = C_0 + k_1 t_I erfc\left[\frac{(X-\Delta X)\sqrt{1-m}}{2\sqrt{D_r t_r^m\left[(t_e+t_{e0})^{1-m}-(\Delta t_{eq\wedge I}+t_{e0})^{1-m}\right]}}\right] \tag{25}$$

On the other hand, with a square root increasing surface chloride concentration during period 1, the chloride concentration in period 2 is given by:

$$C''_{II} = C_0 + k_2 t_I^{0.5} erfc\left[\frac{(X-\Delta X)\sqrt{1-m}}{2\sqrt{D_r t_r^m\left[(t_e+t_{e0})^{1-m}-(\Delta t_{eq\wedge I}+t_{e0})^{1-m}\right]}}\right] \tag{26}$$

Likewise, in period 3, an equivalent exposure time for period 3 ($t_{eq\wedge II}$) having a similar profile at the joint time with period 2 is introduced: $t_{eq\wedge II} = t_e - \Delta t_{eq\wedge II}$, where $\Delta t_{eq\wedge II}$ is the time difference between period 3 and period 2 with matching chloride profiles (year). With a linearly increasing surface chloride concentration during period 1, the chloride concentration in period 3 is given by:

$$C'_{III} = C_0 + k_1 t_I erfc\left[\frac{(X-\Delta X)\sqrt{(t_{II}+t_{e0})^m}}{2\sqrt{D_r t_r^m\left(t_e-\Delta t_{eq\wedge II}\right)}}\right] \tag{27}$$

On the other hand, with a square root increasing surface chloride concentration during period 1, the chloride concentration in period 3 is given by:

$$C'_{III} = C_0 + k_2 t_I^{0.5} erfc\left[\frac{(X-\Delta X)\sqrt{(t_{II}+t_{e0})^m}}{2\sqrt{D_r t_r^m\left(t_e-\Delta t_{eq\wedge II}\right)}}\right] \tag{28}$$

4.2 Service life design of highway tunnel

The first example is the service life design of a highway tunnel with reinforced concrete box structure. The concrete has design strength grade of C40. Two mix compositions are considered in the design stage: Mix A which contains 20% pulverized fuel ash by mass as cement replacement; and Mix B which contains 30% ground granulated blastfurnace slag by mass as cement replacement. The slabs and walls have thickness of 400 mm and the cover to reinforcement is 50 mm except for particular sections of the top slab where the cover is 40 mm. The threshold chloride concentration is taken as 0.06%. The following assumptions are made: a) the surface chloride concentration increases linearly from initial value of 0.01% at start of exposure with 0.018% gradient throughout a build-up period of 3 years; b) the chloride diffusivity decreases with time from value of 5.6×10^{-12} m^2/s for Mix A and 3.7×10^{-12} m^2/s for Mix B at age of 28-day up to an age of 25 years; and c) the instantaneous age factor m for Mix A and Mix B are respectively 0.360/s and 0.371/s. The design life of the tunnel is 100 years and the model predicts the chloride diffusion at 90-year of age, i.e. a corrosion propagation period of 10 years is considered. Figure 2 depicts the assessment results. Both concrete mixes are satisfactory in terms of durability performance. It can be seen that at 90-year age, the threshold chloride concentration reaches only circa 5 to 6 mm and there is no risk of corrosion with a concrete cover of 40 or 50 mm.

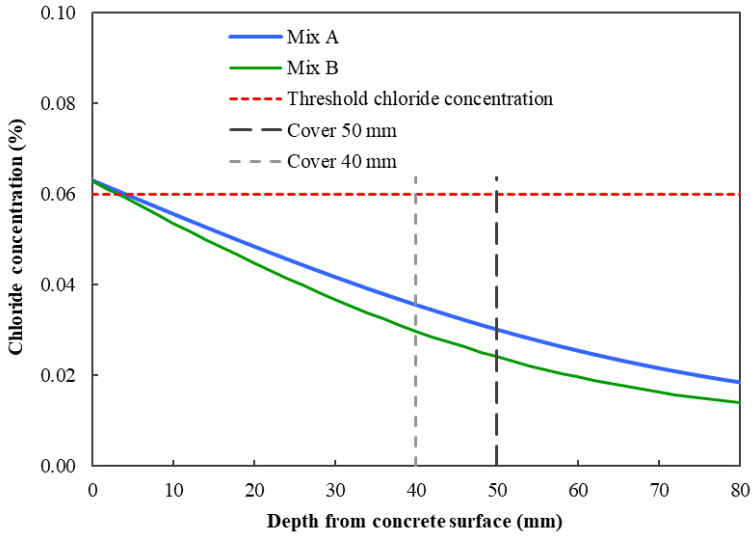

Figure 2: Chloride modelling for different concrete mixes

4.3 Service life checking of temporary haul tunnel

The second example is a temporary haul tunnel of reinforced concrete box structure. The concrete is an ordinary Portland cement concrete mix of grade C40 and the value of m is taken as 0.2. The cover to reinforcement is 45 mm. The threshold chloride concentration is taken as 0.06%. The following assumptions are made: a) the surface chloride concentration increases in square root manner from initial value of 0.005% at start of exposure throughout a build-up period of 7.5 years; b) the gradient of square root increasing surface chloride concentration k_2 is 104.46×10^{-6} $/s^{0.5}$; and c) the chloride diffusivity decreases with time from value of 3×10^{-12} m^2/s at age of 56-day up to an age of 25 years. The design life of the temporary tunnel is 30 years and the age of modelling is 24 years to check and identify any risk of corrosion in the remaining years of usage. Figure 3 depicts the assessment results. It can be seen that the depth of threshold chloride concentration reaches circa 28 mm and there is no risk of corrosion with a concrete cover of 45 mm.

Proceedings DOI: 10.21467/proceedings.171
ISBN: 978-81-970666-7-2

Series: AIJR Proceedings
ISSN: 2582-3922

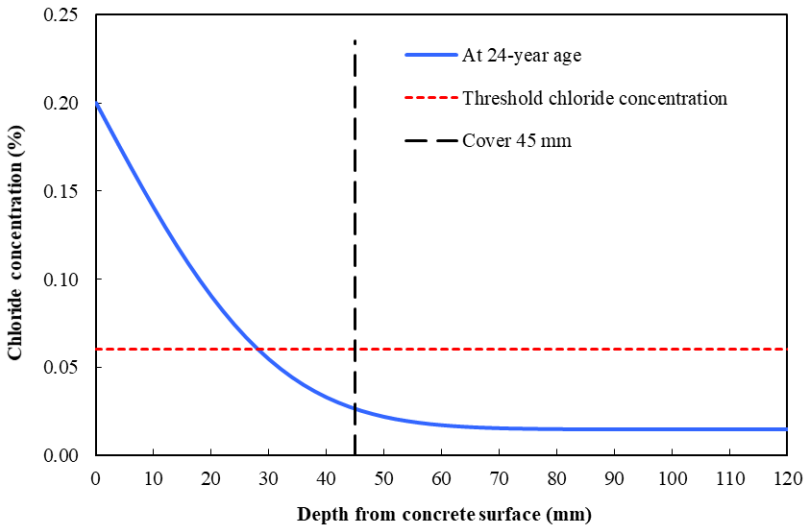

Figure 3: Chloride modelling for temporary haul tunnel

5 CONCLUSIONS

In this paper, analytical models of chloride ion diffusion have been devised, with explicit formulations to account for the effects of time-variation of chloride diffusivity of concrete, time-variation of surface chloride concentration, and temperature. The accuracy of the analytical models is highly dependent on the model input. Experimental measurements to establish the chloride diffusivity of concrete by way of migration cell experiment, accelerated chloride penetration, non-steady-state migration experiment, and rapid chloride permeability test have been outlined. Examples of durability assessment of reinforced concrete tunnels are presented to demonstrate the applications of the chloride diffusion model.

APPENDIX

A.1 Error function

The error function, denoted by *erf*, is defined as:

$$erf(z) = \frac{2}{\sqrt{\pi}} \int_0^z e^{-t^2} dt \qquad \text{(A1)}$$

Mathematically, the error function represents the area under the Gaussian probability density function $2e^{-t\wedge 2}/(n)^{0.5}$ for $t \in [0, z]$, where $erf(\infty) = 1$. The complementary error function, denoted by *erfc*, is defined as:

$$erfc(z) = 1 - erf(z) = \frac{2}{\sqrt{\pi}} \int_z^\infty e^{-t^2} dt \qquad \text{(A2)}$$

There exist various numerical approximations of the error function, for example:

$$erf(z) \approx 1 - \frac{1}{\sqrt{\pi} z} e^{-z^2} \qquad \text{(A3)}$$

A.2 Volhard titration

The methodology and procedures of Volhard titration are detailed in NT Build 208 (Nordtest 1996). To start with, the concrete sample is ground to < 0.1 mm particle size. Approximately 5 g of ground sample is placed into a glass bottle and dried at 105°C and weighed. Distilled water and concentrated nitric acid are added respectively to the bottle and shaken. The solution is then filtered and rinsed twice with 1% nitric acid. Silver

nitrate ($AgNO_3$) solution is added in excess from the burette, followed by 2 to 3 ml of benzyl alcohol (C_7H_8O) or nonanol ($C_9H_{20}O$) and 1 ml of saturated ammonium ferri-sulphate solution ($NH_4Fe(SO_4)_2 \times 12H_2O$). A stopper is then inserted to the bottle followed by vigorous shaking to separate the silver nitrate. The remaining amount of silver nitrate is titrated with ammonium thiocyanate solution (NH_4SCN) with intensive mixing until the solution attains a permanent weakly red colour (formation of $FeSCN^{2+}$). The chloride ion content is determined from the silver ion content minus the thiocyanate ion content.

PUBLISHER'S NOTE

AIJR remains neutral with regard to jurisdictional claims in published maps & institutional affiliations.

HOW TO CITE

Ng *et al.* (2024). Analytical Chloride Diffusion Model for Durability Assessment of Concrete-Lined Tunnels. *AIJR Proceedings*, 166-177. https://doi.org/10.21467/proceedings.171.15

REFERENCES

AASHTO 2007. *Standard Method of Test for Electrical Indication of Concrete's Ability to Resist Chloride Ion Penetration*. *AASHTO T 277*, American Association of State Highway and Transportation Officials, Washington DC, USA.

Angst, U. & Vennesland, Ø. 2009. Critical chloride content in reinforced concrete – state of the art. In M.G. Alexander, H.-D. Beushausen, F. Dehn & P. Moyo (ed.), *Concrete Repair, Rehabilitation and Retrofitting II: Proceedings, 2nd International Conference on Concrete Repair, Rehabilitation and Retrofitting*. *Cape Town, 24-26 November 2008*. Taylor & Francis Group: 311-317.

Bamforth, P. 2004. *Enhancing Reinforced Concrete Durability*. *Technical Report 61*, Concrete Society, Surrey, UK.

Buildings Department 2013. *Code of Practice for Structural Use of Concrete*. Buildings Department, Hong Kong.

CEN (European Committee for Standardization) 2013. *EN 206: Concrete - Specification, Performance, Production and Conformity*. European Committee for Standardization, Brussels.

CEN (European Committee for Standardization) 2023. *EN 1992: Eurocode 2 - Design of Concrete Structures: Part 1-1: General Rules and Rules for Buildings, Bridges and Civil Engineering Structures*. European Committee for Standardization, Brussels.

Crank, J. 1975. *The Mathematics of Diffusion*. Clarendon Press, London, UK.

Freedman, D. 1983. *Brownian Motion and Diffusion*. Springer-Verlag, New York, USA.

Gjørv, O.E. 2014. *Durability Design of Concrete Structures in Severe Environments*. Second edition. CRC Press, Boca Raton, USA.

Hooton, R.D. 2014. Achieving concrete durability for specified service-life in chloride exposures. In S.O. Ekolu, M. Dundu & X. Gao (ed.), *Construction Materials and Structures: Proceedings of the First International Conference on Construction Materials and Structures. Johannesburg, 24-26 November 2014*. IOS Press: 3-15.

Hooton, R.D., Pun, P., Kojundic, T. & Fidjestol, P. 1997. Influence of silica fume on chloride resistance of concrete. In L.S. Johal (ed.), *Proceedings of International Symposium on High-Performance Concrete. New Orleans, 20-22 October 1997*. Precast/Prestressed Concrete Institute: 245-249.

Japan Society of Civil Engineers 1999. *Standard Specification for Design and Construction of Concrete Structures*. Japan Society of Civil Engineers, Tokyo.

Laidler, K.J. 1984. The development of the Arrhenius equation. *Journal of Chemical Education*, 61(6): 494-498.

Mauro, J.C. 2021. *Materials Kinetics: Transport and Rate Phenomena*. Elsevier, Amsterdam, Netherlands.

Mehta, P.K. & Monteiro, P.J.M. 2014. *Concrete: Microstructure, Properties, and Materials*. Fourth edition. McGraw-Hill Education, New York, USA.

Nordtest 1996. *NT Build 208: Concrete, Hardened: Chloride Content by Volhard Titration*. Nordic Council of Ministers, Espoo.

Nordtest 1997. *NT Build 355: Concrete, Mortar and Cement-based Repair Materials: Chloride Diffusion Coefficient from Migration Cell Experiments*. Nordic Council of Ministers, Espoo.

Nordtest 1995. *NT Build 443: Concrete, Hardened: Accelerated Chloride Penetration*. Nordic Council of Ministers, Espoo.

Nordtest 1999. *NT Build 492: Concrete, Mortar and Cement-based Repair Materials: Chloride Migration Coefficient from Non-steady-state Migration Experiments*. Nordic Council of Ministers, Espoo.

Page, C.L., Shott, N.R. & El Tarras, A. 1981. Diffusion of chloride ions in hardened cement pastes. *Cement and Concrete Research*, 11(3): 395-406.

Shi, C.J., Yuan, Q., He, F.Q. & Hu, X. 2020. *Transport and Interactions of Chlorides in Cement-based Materials*. CRC Press, New York, USA.

Spiechowicz, J., Marchenko, I.G., Hänggi, P. & Łuczka, J. 2023. Diffusion coefficient of a Brownian particle in equilibrium and nonequilibrium: Einstein model and beyond. *Entropy*, 25(1): 42.

Tang, L. & Gulikers, J. 2007. On the mathematics of time-dependent apparent chloride diffusion coefficient in concrete. *Cement and Concrete Research*, 37(4): 589-595.

Tang, L. & Nilsson, L.-O. 1992. Chloride diffusivity in high strength concrete at different ages. *Nordic Concrete Research*, 11(1): 162-171.

Wang, J., Ng, P.L., Wang, W.S., Du. J.S. & Song, J.Y. 2017. Modelling chloride diffusion in concrete with influence of concrete stress state. *Journal of Civil Engineering and Management*, 23(7): 955-965.

Wang, J., Ng, P.L., Su. H. & Du, J.S. 2019. Meso-scale modelling of stress effect on chloride diffusion in concrete using three-phase composite sphere model. *Materials and Structures*, 52(3): 55.

Wang, J., Ng, P.L., Su, H. & Du, J.S. 2020. Influence of the coupled time and concrete stress effects on instantaneous chloride diffusion coefficient. *Construction and Building Materials*, 237: 117645.

Zhou, S. 2014. Modelling of chloride diffusion with linear increase of surface chloride concentration. *ACI Materials Journal*, 111(5): 483-490.

Zhou, S. 2016. Analytical model for square root increase of surface chloride concentration and decrease of chloride diffusivity. *Journal of Materials in Civil Engineering, ASCE*, 28(4): 04015181.

Zhou, S. 2018. Relationships of diffusivities and age factors between analytical and empirical chloride models for decreasing diffusivities. In T.B. Sui, T.C. Holland, Z.M. Wang & X.L. Zhao (ed.), *Proceedings of 14th Conference on Recent Advances in Concrete Technology and Sustainability Issues. Beijing, 28 October-2 November 2018. ACI Special Publication, SP-330*, American Concrete Institute: 55-66.